CHALMERS
UNIVERSITY OF TECHNOLOGY

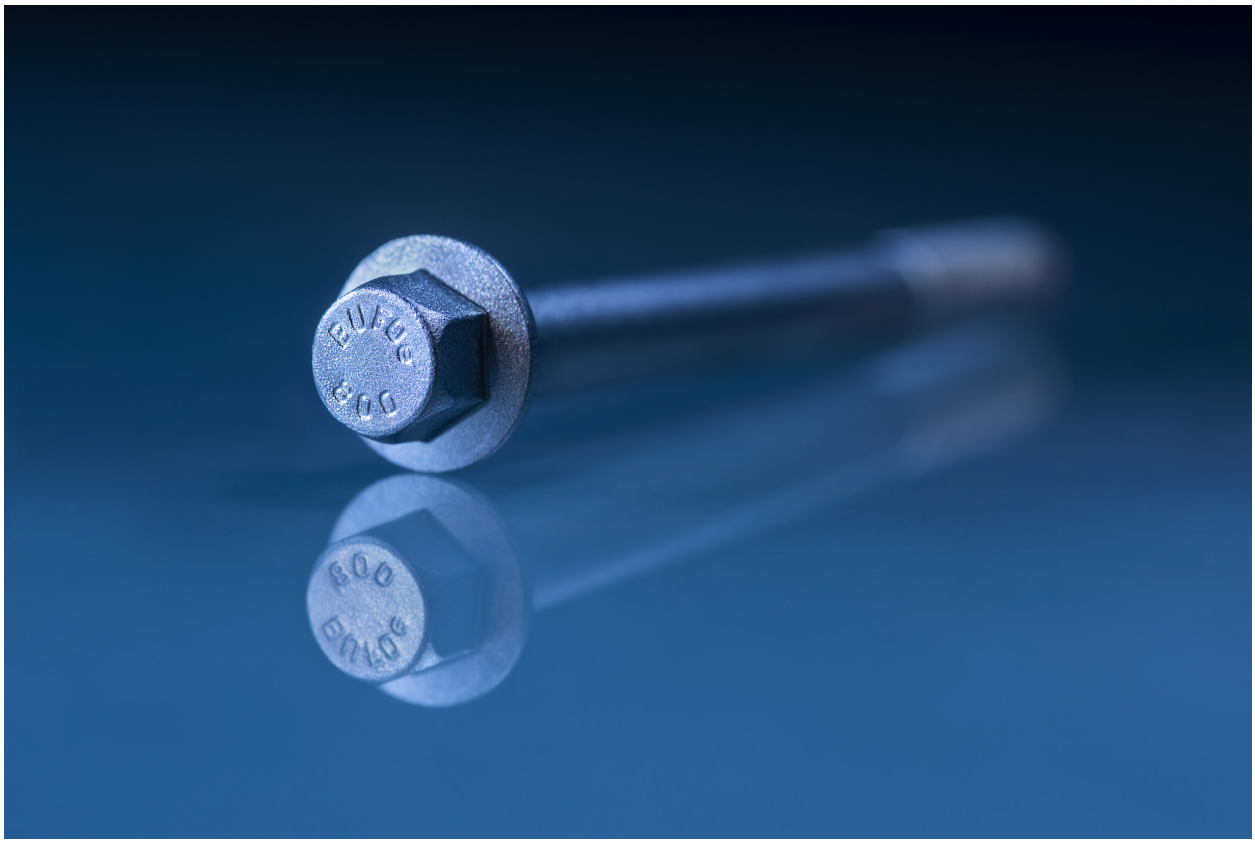

Investigating the effect of work hardening on fatigue performance of fastener steels

Master's thesis in Master Programme Materials Engineering

FABIAN SOMI, MATTIAS WALLDÉN

DEPARTMENT OF INDUSTRIAL AND MATERIALS SCIENCE

CHALMERS UNIVERSITY OF TECHNOLOGY
Gothenburg, Sweden 2023
www.chalmers.se

Master's thesis 2023

Investigating the effect of work hardening on fatigue performance of fastener steels

FABIAN SOMI, MATTIAS WALLDÉN

CHALMERS
UNIVERSITY OF TECHNOLOGY

Department of Industrial and Materials Science
Division of Engineering Materials
Chalmers University of Technology
Gothenburg, Sweden 2023

Investigating the effect of work hardening on fatigue performance of fastener steels
FABIAN SOMI, MATTIAS WALLDÉN

Supervisor: Emmy Pavlovic, Bulten AB
Examiner: Johan Ahlström, Department of Industrial and Materials Science

Master's Thesis 2023
Department of Industrial and Materials Science
Division of Engineering Materials
Chalmers University of Technology
SE-412 96 Gothenburg
Telephone +46 31 772 1000

Cover: BUFOe fastener

Typeset in LaTeX
Printed by Chalmers Reproservice
Gothenburg, Sweden 2023

Investigating the effect of work hardening on fatigue performance of fastener steels
FABIAN SOMI, MATTIAS WALLDÉN
Department of Industrial and Materials Science
Chalmers University of Technology

Abstract

Bulten group aims to introduce a new line of high performance fasteners, manufactured without the conventional energy intensive heat treatment process. This thesis aims to answer how this highly work hardened material performs with respect to fatigue life. Drawn rods with differing degrees of work hardening were subjected to tensile and fatigue testing. Due to the importance of the surface properties in the material a novel method of notching using an indentation tool was performed.

The results indicate an increase in fatigue life for the further work hardened material at elevated loads, likely due to the increase in strength. At lower loads the results show no difference and an increased spread in number of cycles to failure. When the influence of a increase in monotonic yield strength is correct for by relating it the applied stress amplitude, the less drawn material performs better. Finally the possibility of using a Junker vibration testing machine for determining fatigue properties is investigated.

Keywords: Fatigue, work hardening, fasteners, fractography, mechanical testing

Acknowledgements

We the authors would like to thank our supervisor Emmy Pavlovic for her constant support of the project, and special mention to her extensive knowledge of fasteners and their production processes which was invaluable for this thesis. In addition we would like to thank the whole team at Bulten Advanced Technology Center for their guidance and assistance throughout the project. With special mention of Joakim Ericson for his aid in designing the notching tool and Janne Rantamäki for his aid with the notching process and Junker testing. Without their consistent support and encouragement of our work, the final results would not have been possible. Furthermore we would like to extend our gratitude for the acquisition of special grips for the fatigue testing machine by Bulten AB which enabled the project itself.

We would also like to thank the support, both theoretical and practical offered by our Examiner Johan Ahlström, who helped ensure that the fatigue testing machine was not only available but also trained and helped us to ensure its continued function throughout the project. In addition the insight and support offered by Johan within the subject of fatigue was invaluable throughout the project.

FABIAN SOMI, MATTIAS WALLDÉN, Gothenburg, June 2023

Nomenclature

ϵ_d	Draw ratio
d	Actual diameter
D	Initial diameter
σ	Stress
σ_m	Mean stress
σ_a	Stress amplitude
σ'_f	Fatigue strength coefficient
σ'_r	Endurance limit
ϵ	Strain
ϵ_p	Plastic component of strain
ϵ'_f	Ductility coefficient
K_t	Stress concentration factor
E	Young's modulus
N_f	Number of cycles to failure
b	Fatigue strength exponent
c	Ductility exponent in fatigue

UTS	Ultimate tensile strength
YS	Yield stress
LCF	Low cycle fatigue
HCF	High cycle fatigue
HV	Vickers Hardness

Contents

1
Introduction

1.1 Background

In the face of the escalating threat posed by climate change, the imperative to reduce carbon emissions from industrial activities has become paramount, underscoring the pivotal role of industries in driving global efforts towards a sustainable future. One of the industrial actors is the fastener producer Bulten. Bulten is striving towards a greener production through their BUFOe project, which aims to eliminate heat treatment in fastener production. Removing the heat treatment process means that strength and other properties must be achieved by other means. For the BUFOe project this is accomplished by increasing the amount of work hardening induced in the fastener material. The objective of this study is therefore to examine the influence of work hardening on fatigue properties to alleviate a present knowledge gap within the BUFOe project.

Fasteners are a vital component of countless products today, used in virtually all industries globally, where they provide mechanical fixation, commonly by the forming of a bolted joint. Most fasteners are produced by a process of wire or rod drawing to a desired circumference, cut to length and then formed in multiple forging steps. Thereafter the threads are formed by rolling the bolt between two ribbed dies.

The traditional bolt production process is then followed by heat treatment, to create the final properties of the bolt. The prescribed heat treatment type is a quench and temper process, as stated in standard ISO-898-1 [1].

The goal of the BUFOe project is to achieve similar properties as current high performance bolts, in grade 8.8 and 10.9 [1] while avoiding the energy intensive heat treatment process. This is done by increasing the amount of work hardening in the material by increased deformation induced by higher amounts of drawing and forging. The difference between the traditional and the BUFOe processes is demonstrated in Fig. 1.1.

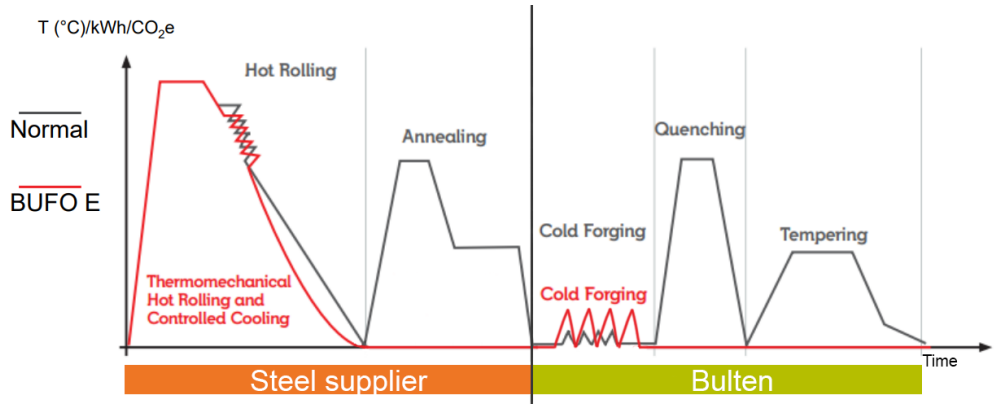

Figure 1.1: Principal heat treatment of standard bolts compared to BUFOe process, provided by Bulten.

1.2 Objective

The aim of this work is to bridge the knowledge gap around fatigue for the BUFOe 800 fastener which uses 22MnB5Ti as its material. The chemical composition is available in Appendix. A.1. The investigation is done by evaluating the fatigue life of varying levels of work hardened material. The target is to aid Bulten in determining the optimal amount of work hardening to be induced during the production of their fasteners. Bulten also wishes to investigate the feasibility of using a Junker's vibration testing machine to perform simplified fatigue testing, which is also added to the scope of this project, this work is included in Appendix B.

The objective is specified down into the following research questions:

-What are the strengths and weaknesses of different methods of testing fatigue life for work hardened material?

-Out of the provided test material, which degree of deformation gives the best fatigue life?

-Is there any correlation between the fracture mode and fatigue life?

-Can trends in fatigue life be evaluated using a Junker's testing machine?

2
Theory

In this chapter the theoretical background of the project is discussed, including the production of the heat treatment free bolts, and the resulting effects on material properties. Finally the theoretical background for fatigue in metals, and testing thereof is covered.

2.1 Fastener production

The production of fasteners is a multiple stage process which is discussed in detail in this chapter. Generally fastener production begins from a wire mounted on a steel spool, being followed by drawing, forging, threading and finishing. This steel wire is produced in a steel mill, in the case of Bulten's BUFOe project this is done by thermomechanical rolling.

2.1.1 Rod drawing

Rod drawing is a process in which a round rod is drawn through a die reducing the cross section. Multiple passes through decreasing die sizes with intermediate annealing heat treatment can be required to reach the final shape and properties. The drawing is an indirect compression process, in which the wire is pulled through the die by tension, however the contact of the die's faces with the material gives rise to compressive stresses inside the material leading to deformation via shear mechanisms. [2]

The relationship between the initial and final diameter of a drawn rod is known as the draw ratio, shown in Eq. 2.1

$$\epsilon_d = 1 - \frac{d^2}{D^2} \qquad \text{(Eq. 2.1)}$$

During the drawing stage the surface grains are orientated in the drawing direction, which is shown in Fig. 2.1. This results in a anisotropic increase in properties such as strength in the axial direction by the aforementioned work hardening [3]. For the BUFOe project the drawing is performed in line with the cold forging machine, as the rod is fed into the machine.

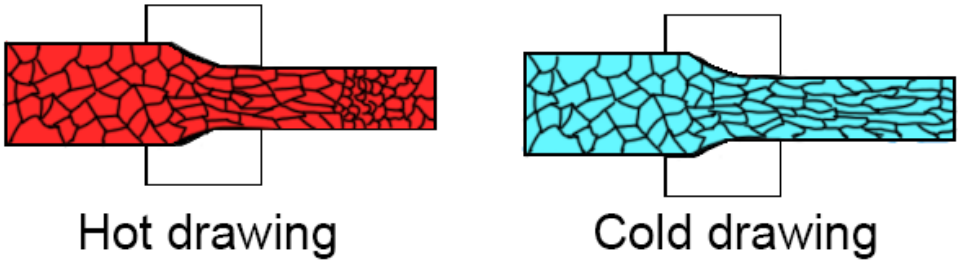

Figure 2.1: Effect of drawing on grain structure, displaying lack of recrystallization during cold drawing.

2.1.2 Cold forging

After the material is drawn to a specified diameter, the rod is cut and cold forging can begin. This is a multiple stage process as illustrated in Fig. 2.2. Starting with a rough shape the head is formed progressively to avoid excessive forming in a single operation. Thereafter the thread is formed, generally done by rolling the fastener between two ribbed dies that produce the threads.

This process generates a significant amount of deformation which in turn results in residual stresses. In the drawing process this is exclusively compressive whereas in the forging steps both compressive and tensile residual stresses can be introduced. To amend these residual stresses and to get a uniform bolt heat treatment is performed in traditional bolts after these steps, however for BUFOe this is not done which leaves a unique final stress distribution in the BUFOe fastener. Careful forging design is required in order to assure uniform work hardening and thereby uniform properties in the BUFOe bolts.

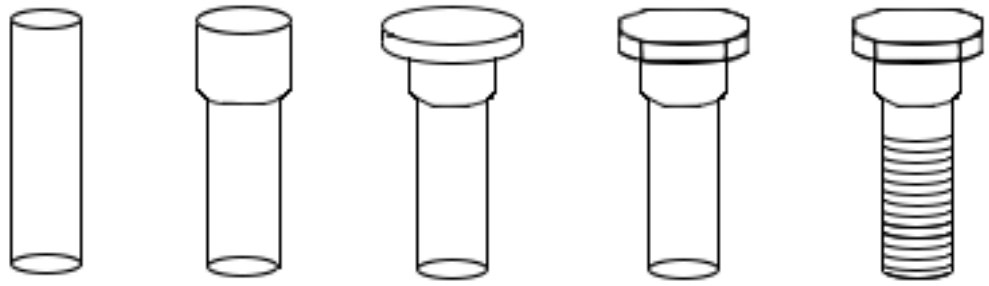

Figure 2.2: Shaping process for a classic fastener, starting from a cut rod.

2.1.3 Sample production

This project uses drawn rods as samples and not BUFOe fasteners, the drawn samples has an increasing amount of drawing in each set, resulting in progressively more work hardening by the rod drawing process. As the samples are not the final fastener, the project does not answer the final fatigue properties of the finished bolts, but only investigated the effect of work hardening on fatigue life, which should correlate to the BUFOe fasteners.

2.2 Work hardening

Work hardening, or dislocation hardening, is the tendency of crystalline materials such as metals, under the effect of plastic deformation to become increasingly resistant to further plastic deformation. This behavior is illustrated the classic stress strain curve, seen in Fig. 2.3 with the increase in strength between points two and one. Work hardening is only one of several strengthening mechanism in metals.

The primary mechanism of plastic deformation in metals is through the movement of dislocations. When a dislocation moves it inevitably interacts with other imperfections, such as different dislocations. As a result of this interaction the mobility of the dislocation is reduced, essentially entangling the dislocations. This in turn requires a greater force to further move the dislocation, in other words the material must be subjected to a larger stress to further deform. Furthermore, the density of dislocations in the material increases by orders of magnitude during plastic deformation [4]. Dislocations may nucleate at grain boundaries, or at incoherent interfaces between the matrix, precipitates and inclusions. If these are absent, dislocations may also nucleate in the homogeneous crystal lattice of the material. The entanglement of dislocations and the increase in dislocation density leads to the observed behavior of increasing hardness with increasing strain, known as work hardening.

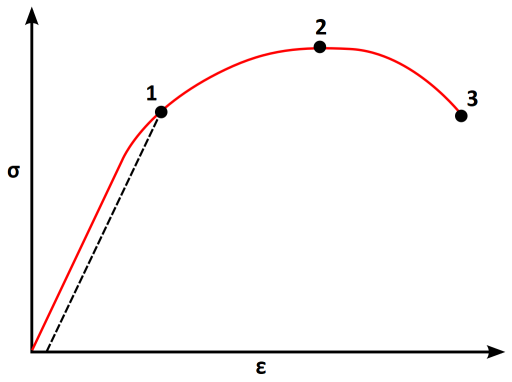

Figure 2.3: Typical engineering stress strain curve, illustrating deformation hardening, with the numbering signifying in numerical order, YS (Yield Stress), UTS (Ultimate Tensile Stress), and fracture.

2.3 Fatigue

Fatigue is the deterioration of some mechanical properties in components undergoing cyclic loading, by a gradual development and growth of cracks. This loss of properties will eventually lead to component failure, with an estimated 90% of component failures in motion being as a result of fatigue. Understanding the fatigue behavior of materials is therefore of critical importance to assure the durability of critical components, which are loaded by a cyclic load (such as fasteners). Fatigue is caused by the initiation and propagation of small cracks under repeated cyclic loading. These cracks continue to grow until they reach a critical size and failure occurs. Fatigue failure commonly occurs at low stress when compared to the material yield strength. [4]

2.3.1 The mechanics of fatigue

Fatigue failure, as with most types of failure, initiates at weak points and stress concentrations in the material, such as sharp edges, scratches and inclusions. Under loading these defects are enhanced by the growth of slip bands. Slip bands are when a certain plane in the metal slips relative to the neighbouring planes, causing surface roughness. The slip bands are caused by the repeated cyclic strain in the material, seen during fatigue especially. In the unlikely scenario of no defect being present, slip bands themselves may serve as a initiation site for cracks to nucleate on. [4]

After the initial stage of crack nucleation, on either a defect or a slip band, the fatigue crack will grow. Initially this occurs at a very small growth per load cycle, as the crack grows along the crystallographic slip planes. The small crack then grows until it encounters a grain boundary. At the grain boundary the crack growth quickens as the dominant crack begins to grow perpendicular to the applied stress, this stage is often separated out into a second stage of primary crack growth. A large portion of the total fatigue life is consumed in the crack initiation and initial growth stage, with the portion of fatigue life consumed in this initial stage varying depending on the mean stress σ_m [4]. At elevated stress levels multiple cracks can form and coalesce to form a larger crack causing a rapid nucleation and initial crack growth stage. For lower stress levels on the other hand fewer or single microcracks propagate into the final fatigue crack causing slower initial crack nucleation and growth. Thereafter depending on the strength of the grain compared to the grain boundary, the crack will either continue as a transgranular or in rare cases as a intergranular fracture.[5] [6]

The anticipated effect of work hardening on the fatigue life of a material is twofold; firstly the deformation is likely to introduce compressive residual stresses into the material, which may increase fatigue life. Secondly the increase in strength achieved by the work hardening process could theoretically result in an increase in fatigue life due to the correlation between mechanical properties such as yield strength, ultimate tensile strength and hardness with fatigue life [7]. Additionally it is probable that the material studied in this work will display anisotropic properties as other papers

has shown similar drawn steels to display anisotropic fatigue strength. [3]

2.3.2 Evaulating fatigue properties

Fatigue testing is typically performed using specialized fatigue testing machines, that can rapidly load and unload a sample at varying speeds and loads. Fatigue testing generally takes many thousands, and up to millions of cycles creating a very extensive process, requiring long time periods to complete. During tensile fatigue testing the applied load typically has a sinusoidal waveform. A typical example of this loading can be seen Fig 2.4. The choice of mean stress, σ_m, determines the form of the testing, i.e tension-compression, tension-tension etc, while stress amplitude σ_a determines the degree of loading.

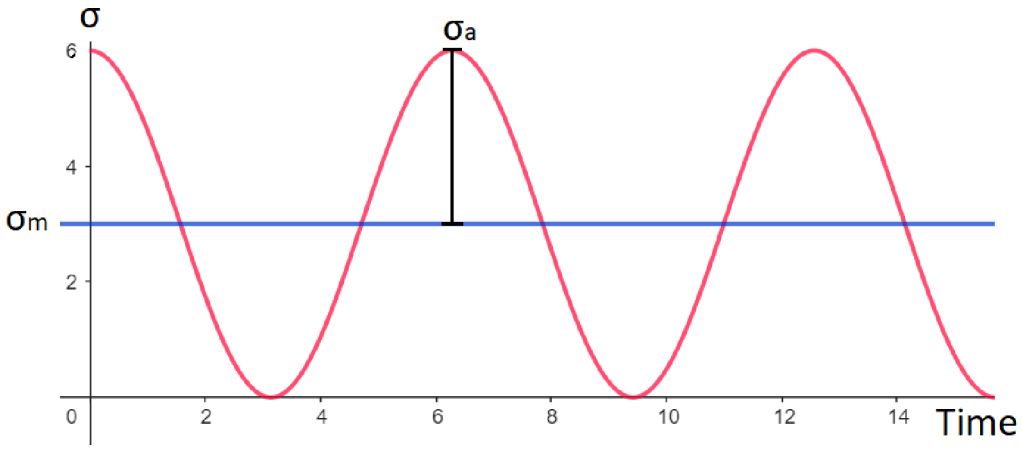

Figure 2.4: Example sinusoidal load, tension-tension in this case, σ_m=mean stress, σ_a=Stress amplitude, R = $\frac{\sigma_{min}}{\sigma max} = 0, \sigma_m = \sigma_a$.

There are several methods of fatigue testing, two of which are; tensile fatigue testing and bending fatigue testing. Tensile fatigue testing has a axially loaded specimen, similar to that of a tensile test but with an alternating load. For bending tests the specimen is mounted in a three or four point bending rig and loaded in pure bending while always being held in tension.

A common type of sample used in high cycle fatigue testing are tensile test specimens, often referred to as a dogbone. However altering the rod by machining may interfere with the final results. As one issue that arises in fatigue testing of the drawn BUFOe rod material, is that during the drawing process the core of the material experiences less deformation resulting in a less work hardened microstructure.

Another common testing geometry is a notched fatigue test. In these samples a notch is added at the center of the test material which causes a stress concentration to ensure fracture occurs within an expected region [4]. For a cylindrical test material this is commonly done by machining a small groove around the materials

center, which would remove a part of the work hardened area in the BUFOe sample.

The three and four point fatigue test can use round specimens and pose some advantages as they require less sample preparation, with the stress being concentrated by the process itself as compared to a tensile test. However it requires a larger investment in the creation of a bending rig, additionally the data given cannot be directly compared with the more common tensile fatigue data. [8]

2.3.3 Interpreting fatigue

Fatigue is generally interpreted using a S-N curve, commonly referred to as a Wöhler curve. A general example of this curve is shown in Fig 2.5 which illustrates the stress (or strain) the material is loaded with, and the number of cycles to failure, N_f. These S-N curves represent the fatigue life, also known as fatigue strength of the material. For a stress-life approach these curves are generated by running repeated cycles until failure occurs at a set stress level. For some materials such as steels, failure may not occur as there exists a stress level below which the material will not fail due to fatigue, this is known as the materials endurance limit (σ_r).

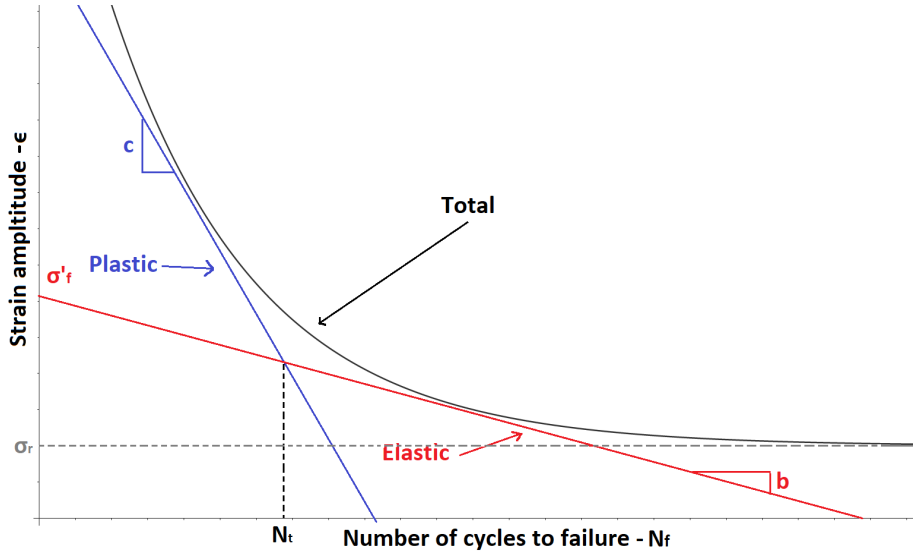

Figure 2.5: Example log-log S-N curve, with the endurance limit, σ_r, and the elastic and plastic fitting lines shown.

The fatigue response of a material can be either elastic or elastic-plastic depending on the severity of the loading. At higher loads, plastic deformation occurs in each cycle, while at lower loads the strain response is purely elastic. The regime where plastic deformation occurs is known as low cycle fatigue (LCF), and where it is absent is known as high cycle fatigue (HCF). The point where the behavior shifts is schematically marked by N_t in Fig. 2.5.

The LCF regime can be described with the Manson-Coffin relationship:

$$\frac{\Delta\epsilon_p}{2} = \epsilon'_f(2N)^c \qquad \text{(Eq. 2.2)}$$

The HCF regime can be described with the Basquin's relationship:

$$E\epsilon_a = \sigma_a = \sigma'_f(2N)^b \Rightarrow \frac{\Delta\epsilon}{2} = \frac{\sigma_a}{E} = \frac{\sigma'_f(2N)^b}{E} \qquad \text{(Eq. 2.3)}$$

The fatigue strength exponent b, and the ductility exponent in fatigue c, represent the slope of the line drawn by each equation in a log-log plot. The fatigue strength coefficient σ'_f, is the stress value of the Basquin curve at $2N = 0$. The same is true of the ductility coefficient ϵ'_f. For a S-N curve covering the whole range of fatigue, Eq. 2.2 & 2.3 may be combined as seen in Fig. 2.5. [4]

2.3.4 Simplified fatigue testing

Determining the chosen loading levels can be done by various methods. A common method for fasteners is the staircase method. In this method a fixed mean stress level is set and then a decreasing or increasing amount of stress amplitude is applied to determine the fatigue endurance limit. If the initial specimen did not fail, the amplitude is increased for the next test specimen. This process is repeated until a test specimen reaches the set run out number of load cycles for the test plan. The run out number is often in the range of $5 * 10^6 - 10^7$ cycles [4]. Finally to ensure a level of statistical certainty a minimum of 6 samples for each chosen stress level should be tested for a preliminary or research study according to appropriate standards [9].

To replace the time intensive staircase method a faster version of fatigue testing is necessary for this investigation due to time limitations. Testing itself will be started at a elevated stress level in the high cycle fatigue region, with the stress amplitude being lowered in a stepwise manner akin to the staircase method, however instead of pursing the fatigue endurance limit a test in the range of 10^6 cycles is the aim. This is chosen as limitations on machine time result in testing beyond this being unfeasible. The tests performed in this stepwise manner will then be used to determine suitable loading levels for each subset of test material to perform a comparative study of the effect of work hardening on fatigue. This method will produce a limited S-N curve while minimizing the need to perform run-out tests.

2.4 Notch effects

Abrupt changes in geometry such as grooves, threads or notches alter the uniform stress distribution and give rise to larger localized stresses during external loading. This is known as a stress concentration [10]. The effect is often visualized by a diagram showing force lines, as seen in Fig. 2.6. The concentration of force lines

between the edges in a rectangular specimen and the hole is illustrated, indicating elevated stress levels at those points in the specimen.

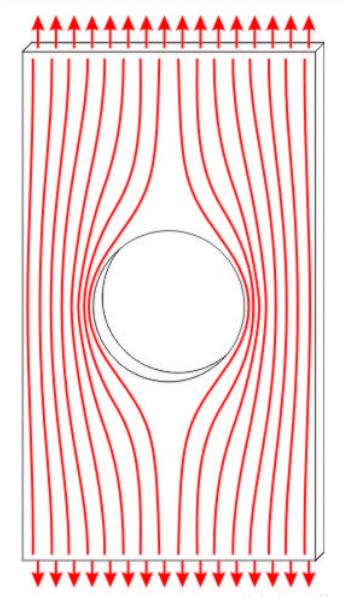

Figure 2.6: Force lines in a specimen with a hole, by Kokcharov licensed under CC BY 3.0.

In mechanical testing, notches are regularly used to control the point at which plasticity or fracture initiates. This is helpful in many instances such as when positioning extensometers. For many common geometries there exists charts to calculate the expected stress concentrations for different notch geometries, expressed as the stress concentration factor K_t [10].

In ductile crystalline materials, such as steels, notch strengthening can be observed meaning that notched samples exhibit a larger E, UTS and strain at fracture than smooth specimens [11]. The difference in elastic stiffness, E, is due to an unnotched sample having a constant cross section while for a notched specimen it is locally smaller. The larger ultimate tensile stress is due to differences in stress states; for an unnotched sample the stress state is uniaxial, while (for the interior of) a notched sample the stress state is triaxial, and a larger force is thus required for yielding. The decrease in area reduction is explained by yielding occurring in the entire specimen (until onset of necking) of the unnotched sample whereas for the notched sample yielding only occurs at the notch, while the rest of the sample remains elastic [12].

3
Methods

In this chapter the various methods used in this thesis are detailed, including test design, sample preparation, tensile and fatigue testing, fractography and finally metallography.

3.1 Test material

Five versions of drawn rods were provided for the invesigation, all drawn from a 9.0mm rod with a different amount of induced deformation, ranging from 10% to 50% as seen in Table. 3.1.
In order to determine the effect of work hardening on fatigue life the bulk of testing was performed on the most and least drawn samples, namely the 10% and 40% drawn rods. The 50% drawn rod had to be excluded due to insufficient griping force with available equipment. Due to the increased strength from work hardening it was important to test each material at a proportional loading level, to ensure that the effect of work hardening is compared and not the higher strength. As such to measure the effect of work hardening a percentage of the yield stress of the given test sample is to be used.

Table 3.1: Table over samples available for testing.

Specimen	Reduction [%]	Dimension [mm]	Area [mm^2]	Draw Ratio
1	11	8.49	56.6	0.21
2	23.9	7.85	48.4	0.42
3	28.5	7.61	45.5	0.49
4	40.4	6.95	37.9	0.64
5	49.4	6.4	32.2	0.74

3.2 Sample preparation

In order to ensure that failure of the test specimens occurs in a repeatable manner, and to avoid failure in the grips, it was necessary to notch the samples. Since preparing a cylindrical dogbone would result in a significant portion of the outer material being removed, which may in turn significantly change the performance of the BUFOe material. As such the standard fatigue testing specimen shape is considered unsuited to the test material provided for this investigation.

An indenting tool was fabricated with the help of Bulten for use with an electro-mechanical testing machine. The geometry of the tool can be seen in Appendix. A.1, with a picture of the tool itself in Appendix. A.2. The tool itself was quenched and tempered to a hardness of 450 HV as the raw material itself lacked sufficient hardness not to deform during the notching process.

The resulting test samples were cylindrical in shape, with a length of 120 mm and a single 1 mm deep indent, as seen in Fig. 3.1.

Figure 3.1: Photograph of notched sample.

A further complication of the chosen notching process was the varying properties and diameters of the testpieces. As such, getting proportional notches between the varying sizes of test material was highly difficult. It was decided to create notches of the same size, with 1 mm of depth in all of the samples. This resulted in a larger proportional notch for the increasingly drawn, and thus smaller cross sectional area specimens.

Due to the determination of the exact notch geometry and the resulting stress concentration factor proving to be very difficult, the decision to calculate engineering stress from the nominal, unnotched diameter was made. As such, unless otherwise specified, any stress given in this report is the engineering stress calculated using the area of the samples before notching.

To measure the consistency of the notching process a series of notched samples were measured using a Mitutoyo PJ300 profile projector. The test series displayed a small variance of 0.1 mm in notch depth, with a probable cause being a small variance in force during the indenting process and human error in the measuring process. The table for this measured data can be seen in Appendix. A.3.

3.3 Tensile testing

To exclusively compare the effect of work hardening on fatigue it was important to load all material proportional to their strength. A increase in mechanical properties can show a trend of increased fatigue properties as discussed previously in Chapter 2.3.1 [7]. Due to this, tensile testing was necessary to determine mechanical properties.

Tensile testing was performed using an Instron 8501 servo-hydraulic load frame to determine the yield and ultimate stress of each test material, both in the notched and unnotched state. On the notched samples the extensometer was placed on the opposite side of the notch in order to record strain after the onset of necking.

The elastic modulus E, is the slope of the elastic portion of the stress-strain curve. The ultimate tensile strength UTS, is naturally the largest recorded stress. The yield strength $R_{p0.2}$ is determined by the intersection of the stress-strain curve and the line with the slope E offset by 0.2% [4]. Multiple tests were performed for each material, and the mean of the results seen in Tab. 4.1. Due to difficulties with the unnotched samples breaking in the grips and no direct relevance to the present work, strain at fracture was not measured for any of the samples.

3.4 Fatigue testing

To replace the time intensive staircase method a faster version of fatigue testing was necessary for this investigation due to time limitations. Testing itself was started at a elevated stress level in the high cycle fatigue region, with the stress amplitude being lowered in a stepwise manner akin to the staircase method, however instead of pursing the fatigue endurance limit a test in the range of 10^6 cycles was the aim. This was chosen as limitations on machine time result in testing beyond this being unfeasible. The tests performed in this stepwise manner were then be used to determine suitable loading levels for each subset of test material to perform a comparative study of the effect of work hardening on fatigue. This method produced a limited S-N curve while minimizing the need to perform run-out tests. Fatigue testing itself was performed in the Instron 8501 machine.

The samples were manually mounted in the machine with the grip bolts torqued to 40 Nm in both lower and upper grips, as can be seen in Fig. 3.2. Thereafter the machine was unloaded to 0 kN and loaded with an oscillating load between 0 kN and the chosen percentile of yield stress for the test, resulting in a σ_m of half of the set upper load. The test was run at 20 Hz, with a sinusoidal waveform under room temperature until fracture was achieved.

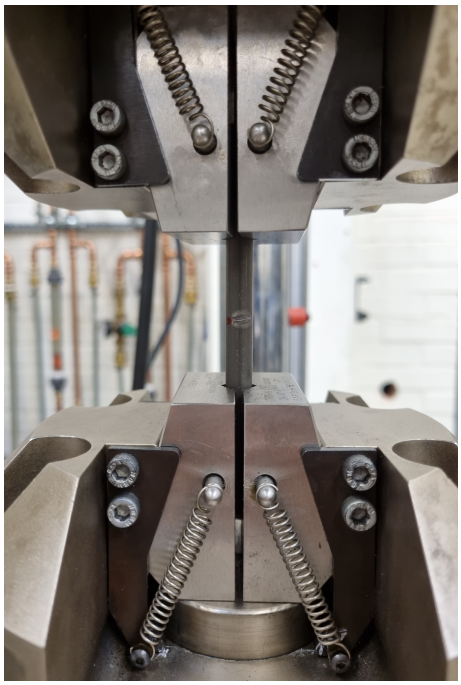

Figure 3.2: Sample mounted in the Instron 8501 fatigue testing machine.

A initial test series was performed to identify suitable loading levels for the various test pieces, starting with the 10% drawn test piece. Multiple tests were run with a σ_m initially at 80% of the materials yield stress. Thereafter tests were carried out at 70%, 60%, 50% and 40% of the materials yield stress. The final loading level of 40% yield stress resulted in intact specimens after over 6.1 million cycles and due to the limited time and frequency available with the Instron fatigue machine the test was marked as a run-out [9]. This process was then repeated for the 40% drawn test pieces, excluding the 40% yield stress test due to the previous run-out. Due to time limitations available for fatigue testing sample size recommendations from standards such as ASTM-E739 was hard to achieve. Therefore the tests were more comparative with a smaller sample size.

3.5 Fractography & microstructure analysis

After completing the fatigue testing the fracture surfaces of the test samples were visually inspected and separated into groups dependent on the determined fatigue initiation site. A subset of these samples were then investigated with stereo microscopy for more detailed analysis, to compare the initiation sites and the size of the fracture surface.

Thereafter micrography samples were created from untested rods to investigate differences in microstructure between the degrees of drawing and the effect of the

notching process on the microstructure of the test material. These samples were cut using an IsoMet precision cutter. Thereafter the cut samples were ground and polished in successive steps using a MetaServ 250, with a final stage of 1 μm polishing diamonds before etching in 3% Nital solution for 3 seconds. The samples were then placed under a microscope to analyze the microstructure of the varying samples, using objective lenses from 2x to 50x magnification.

4
Results

In this chapter the results from the various tests are compiled and shown to the reader. These include results from the tensile and fatigue testing, alongside interpretations of fractography and optical microscopy images.

4.1 Tensile

The results of tensile testing on the 10% and 40% drawn rods without a notch can be seen in Fig. 4.1. The graphs show composite stress/strain curves consisting of multiple tests for each type. More test were performed for the notched samples as these showed a greater variation in the results.

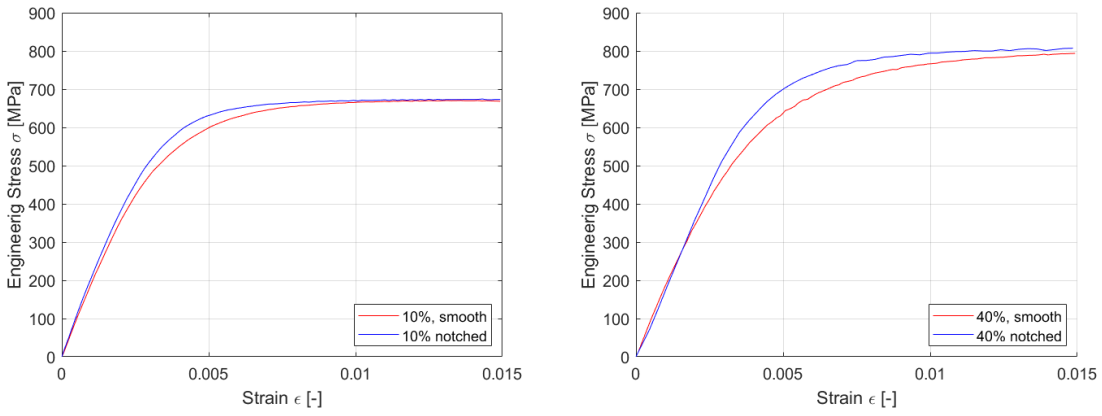

(a) **(b)**

Figure 4.1: Stress strain curves for the 10% (a) and 40% (b) drawn rods in the unnotched states, showing notch strengthening.

The resulting yield and ultimate tensile stresses can be seen in Tab. 4.1. The stresses in Fig. 4.1 were calculated using the same original area for both notched and unnotched samples, indicating that the notch strengthening effect in this case was strong enough to increase the yield strength of the samples.

Table 4.1: Yield and tensile strength data [MPa] for tested materials, values in parentheses are measured values, bold is average.

	10%	10% notched	40%	40% notched
$Rp_{0.2}$	(594,601) **598**	(630,632) **631**	(673,664) **669**	(734,682,757,753,745) **734**
UTS	(673,668) **671**	(673,675) **674**	(806,805) **806**	(807,808,811,811,810) **809**

4.2 Fatigue

The fatigue testing results can be seen summarized in Fig. 4.2, Fig. 4.2a shows a S-N curve for the load as expressed in the percentage of yield stress of the material. Fig 4.2b shows the more typical S-N curve of mean stress as a function of load cycles. The different points are the individual test results shown to indicate the spread of the tests run. To aid visualizing trends in the data, a curve was fitted to each set of tests. As the tests were performed primarily in the HCF regime, the Basquin relationship was chosen to create the curve. The parameters of the Basquin relationship that best match the data were found using nonlinear regression analysis. The obtained values for the parameters are shown in Tab. 4.2. While the Basquin equation is not normally used with a percentage of yield stress, in the present work it still represents the intersection of the curve with the y axis, or the predicted percentage of yield stress at N=0 in the table. This is marked with * in in Table 4.2.

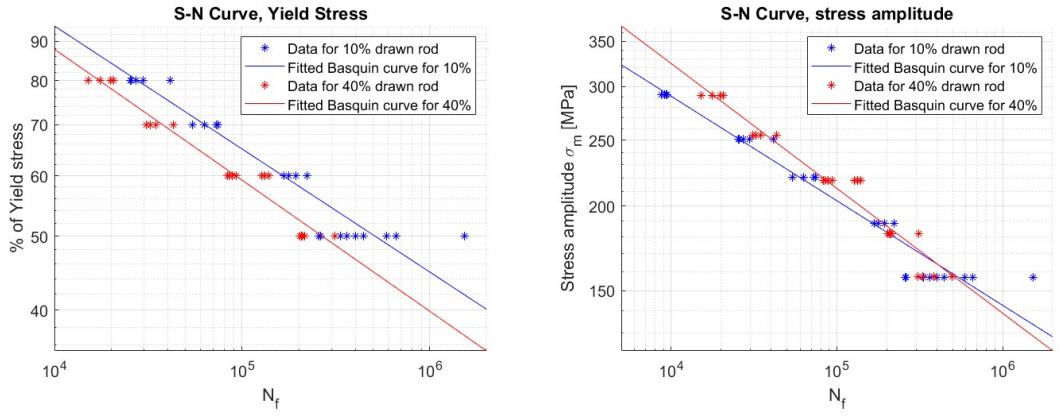

(a) **(b)**

Figure 4.2: S-N curves showing cycles compared to yield stress (a) and stress amplitude (b), 40% drawn rods in red and 10% drawn rods in blue

	10%	40%	10% yield	40% yield
σ'_f	1339.5 MPa	2014.2 MPa	465.35*	481.39*
b	-0.1544	-0.1843	-0.1612	-0.1717

Table 4.2: Obtained values for Basquin relationship parameters

When the load was normalized to a percentage of yield stress as in Fig. 4.2a, the less drawn samples clearly have better fatigue performance over the whole range of testing. When the mean stress is considered as in Fig. 4.2b, the data is less conclusive. While the more drawn sample appears to perform better at higher loads, at lower loads the data presents overlapping and wide distributions.

4.3 Fractography

To better understand the results of the performed fatigue testing the fractograph of the samples tested are of great interest. This is shown and interpreted in this chapter.

The varying zones of the fracture surface are indicated in Fig. 4.3a, being in order, the fatigue crack propagation zone (1), a continuing fatigue crack propagation zone as the growth direction turns (2) and finally the fast fracture zone (3). The initiation site can be estimated by identifying the central point of the fatigue crack propagation zone, which is the brighter part of the fracture surface. After reaching a critical point of surface area for the sample the crack propagation turns and speeds up, until it reaches the final zone where rapid facture occurs. These zones are akin to those shown by ASM handbooks for mild to severe stress concentrations [13].

As can be seen in Fig. 4.3 the initiation site vary between the different samples. At higher loads the initiation site tends towards the center of the notch, while at lower loads the fracture types increasingly vary between the center, halfway to the edge and at the edge of the notch itself. For tests at the same percentile of yield stress where both edge and central initiation sites occur a edge crack initiation becomes more likely at a higher cycle number. For the 40% drawn rods at a load of 50% YS a corner crack initiation resulted in a on average doubling of the cycles to failure. The fatigue initiation point as determined by fractography is available in Appendix. A.2.

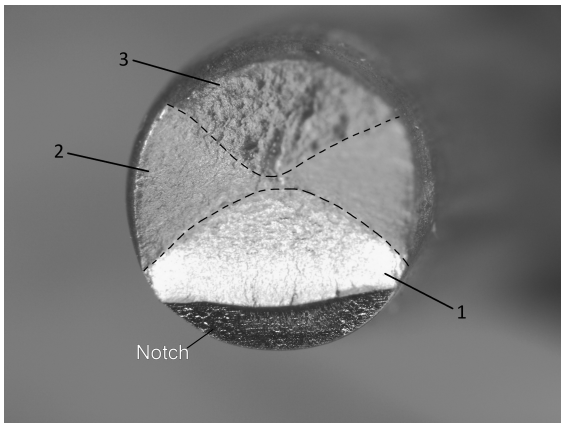

(a) Fatigue initiation at notch center, run at 80% YS. With zones numbered.

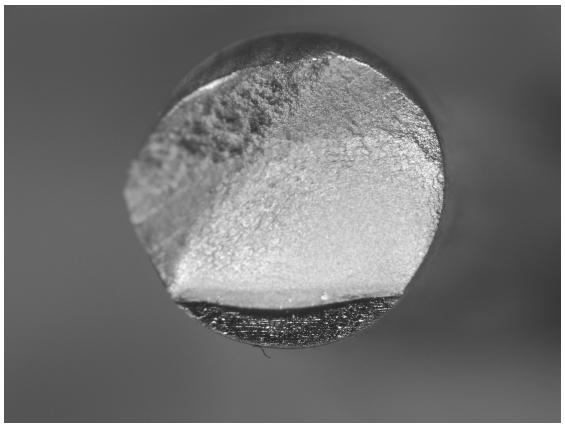

(b) Fatigue initiation at notch edge, run at 60% YS.

(c) Fatigue initiation at left side of notch center, run at 60% YS.

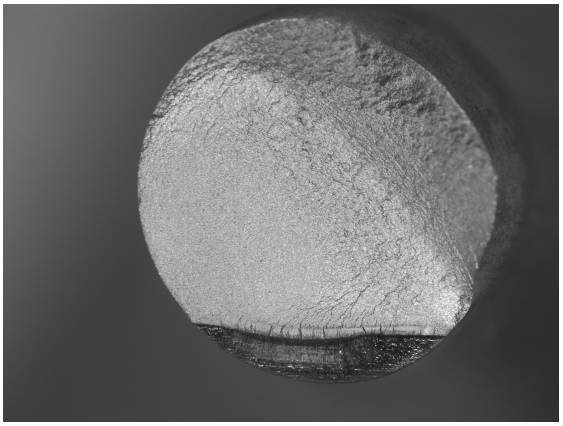

(d) Fatigue initiation at notch edge, run at 50% YS.

Figure 4.3: Comparison of fracture surfaces of a selection of different samples.

4.4 Microscopy

Analysis performed under an optical microscope allowed for an in depth viewing of both the microstructure and the effects of the notch on the surrounding material.

The magnified view seen in Fig. 4.4 shows the 40% drawn specimens (left) and 10% drawn specimens (right) at different magnifications. The expected light ferrite and dark pearlite grains of the material are clearly visible. These grains are significantly elongated in the drawn direction, as expected from the drawing process. A tightening in the distribution of pearlitic bands can be seen in the 40% drawn rods, as the higher amount of drawing results in further elongated bands, most clearly shown in Fig. 4.4e and 4.4f. The effect of the compressive stresses introduced during the notching process is also clearly displayed as the tightened and curved pearlitic bands behind the notch. Dark spheres can be seen in several micrographs, these are likely a type of inclusion formed by one of the carbide forming elements in the steel, such as titanium. A clouseup of these inclusions can be seen in Appendix. A.3.

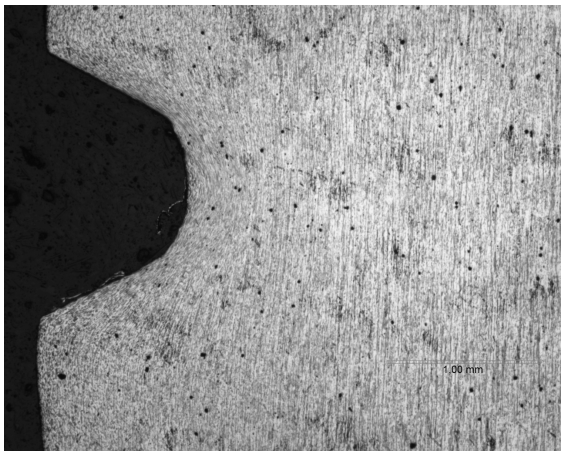

(a) 40% drawn notch overview at 2x magnification

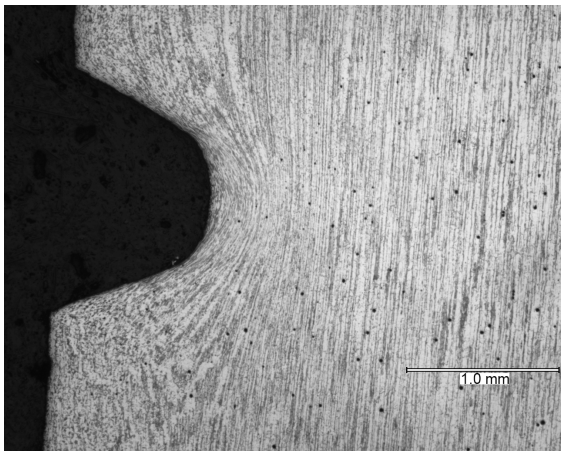

(b) 10% drawn notch overview at 2x magnification

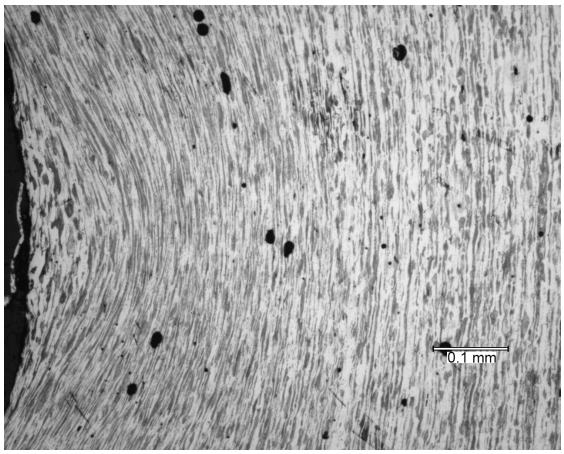

(c) 40% drawn, center of notch view at 10x magnification

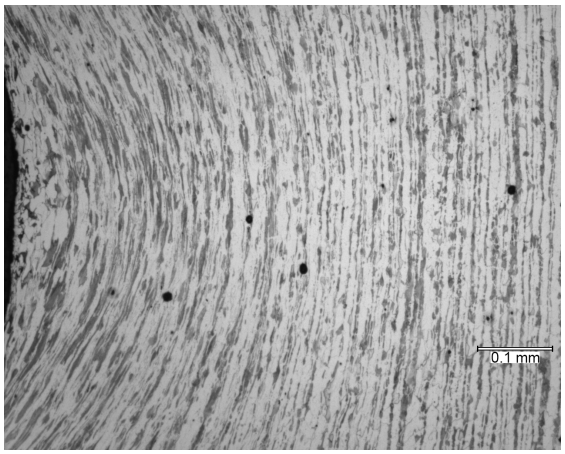

(d) 10% drawn, center of notch view at 10x magnification

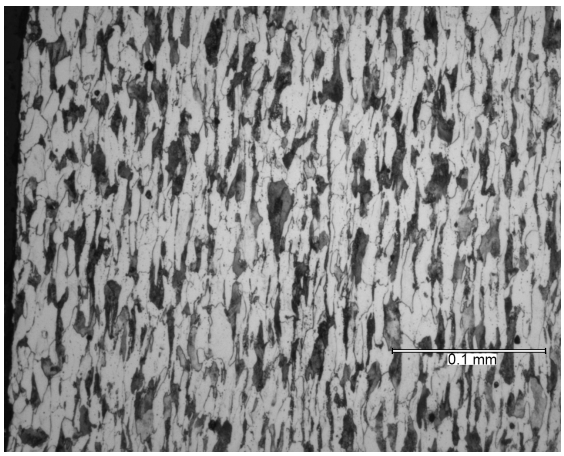

(e) 40% drawn, microstructure near edge of rod away from the notch, view at 20x magnification

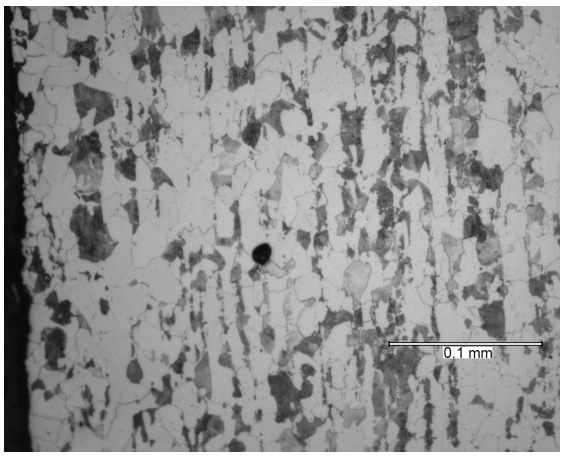

(f) 10% drawn, microstructure near edge of rod away from the notch, view at 20x magnification

Figure 4.4: Overview and comparison of the notched region for 40% (left column) and 10% drawn rods (right column).

5
Discussion

In this chapter the methods used and the results obtained are discussed and further interpreted. With special focus on the interpretation of the fatigue tests and to potential error sources in the executed work.

5.1 Fatigue result interpretation

The results obtained from the fatigue testing of this investigation are in line with the correlation between mechanical properties of strength and hardness with fatigue life at higher loads [7]. However at lower loads the different materials intersect and overlap for the mean stress graphs, see Fig. 4.2b. Hence, at lower dynamic loads and higher number of cycles to failure the amount of work hardening may not have a significant impact. At lower loads and higher cycles, the sensitivity of the samples to imperfections is expected to increase, potentially explaining the larger spread of data. Furthermore the increased time required for each test means performing larger numbers of tests is resource intensive. This overlap in fatigue life may be beneficial for the fastener, as variation in amounts of work hardening will be present inside the finished fastener. As such dimensioning for fatigue life could be simplified.

For the yield stress graph, seen in Fig. 4.2a there are some potential reasons for the reduction in fatigue life when adjusted for a percentage of yield stress of the 40% vs 10% drawn rods. One of these factors is that the increased drawing generates higher strength and increased hardness for the 40% drawn rods which is expected to give a more brittle behavior. This can lead to faster fatigue crack propagation, potentially explaining why the less drawn samples performed better in fatigue.

The drawing process creates a large increase in yield stress and a smaller increase in UTS for the more work hardened rod. This means that using the yield stress to determine the load may adversely affect the more work hardened rod as it experiences higher loads due to the large increase in yield stress. The higher loads for the 40% drawn rod result in the material being closer to its UTS which could have a negative impact on fatigue life, especially if plastic deformation occurs.

A final factor is that the stress in all samples was determined using the original, unnotched cross section. This was due to difficulty in determining the exact geometry of the notch. As a result, the true stress in each sample will be higher than shown. Furthermore as the more drawn samples have a smaller diameter, as such indenting both samples with the same notch depth is expected to result in a higher true stress in the 40% drawn samples, due to the larger relative size of the notch. Due to the difference in geometry and mechanical properties being linked in the

samples, decoupling the effect of these factors proved difficult.

Focusing on the S-N curves one can see that, certain outlier values show a clear separation from the majority of the data points. The process of test sample preparation where some unavoidable errors may be introduced, such as varying indentation depth and notch orientation. These error sources were minimized by inspection of the samples, measuring the force used for each indentation, and for the final batch measuring the depth of the notches using a profile projector.

Furthermore, human error and the need to execute a fatigue test plan rapidly with limited planning time, resulted in some unsuited samples being included. The outlier sample at 50% YS which lasted for over a million cycle for example, was in post inspection seen to have a misaligned notch. That is a notch not perpendicular to the loading direction. The impact that notch misalignment has on the fracture is unknown, however for this outlier sample the fracture occurred at the edge of the notch. As discussed and shown in Chapter 4.3, if the fracture surface grows perpendicular to the force, as anticipated, more material would need to be overcome before fatigue failure would initiate.

The fracture initiation sites themselves can also be seen as a source of increased spread for the fatigue data points. For test groups at the same load with varying initiation sites, a difference in cycle number was observed, with edge initiation generally resulting in a higher cycle number before fracture. A potential source of this variance is the geometry of the notch tool and the difficulty in getting perfect alignment for each indentation.

The numerous advantages offered by the used notching method is however invaluable for the flexibility it provided, allowing rapid preparation of samples when necessary, enabled the maximum utilization of available machine time. A more complicated and accurate notching process by machining could have resulted in more uniform samples, yet the cost of increased lead time which would drastically have reduced the number of possible tests.

Finally to ensure a measure of statistical certainty a sufficient number of samples must be selected. In an ideal scenario each sample would be gathered at different times from varying suppliers to avoid the test material encompassing only a single batch. Due to the costs associated with this type of sample gathering the provided test material is in a single batch form. This results in a potential source of error that should be considered.

5.2 Future work

To extend the obtained results in this report an extensive fatigue testing series of the completed BUFOe fasteners should be performed. Especially to focus on the effect the cold forging steps may have on fatigue life and not only the drawing steps of the rod. If the impact of work hardening is the primary subject of interest then some

form of three point bending could be ideal as compared to the notching method. Three point bending comes at the cost of increased preparation time yet removes issues associated with the notching process. As the design of a classical tensile test sample is unsuited for work hardened samples these two method are the most feasible.

6
Conclusion

In this chapter the conclusions and answers to the posed research questions, to the extent possible based on the investigation are summarized in a condensed form.

-What are the strengths and weaknesses of different methods of testing fatigue life for work hardened material?

For work hardened materials the viable testing methods are either a notched uniaxial fatigue test as performed in this thesis or a fatigue bending test. The notched fatigue tests imposes difficulties in the creation of a notch, which alters the work hardened surface. It is however simple to perform and the notches can be created in varying ways depending on methods available. They can also be tailored to represent the geometry of threads and more in fasteners. A bending test on the other hand requires no sample preparation and offers uniform tests. To perform these tests a bending rig must be manufactured. However there are some difficulty in comparing bending fatigue data to tensile fatigue data and tensile fatigue data is more relevant to fasteners.

-Out of the provided test material, which degree of deformation gives the best fatigue life?

To ensure sufficient sample size for each test the material series was limited to the 10% and 40% drawn rods. The result show an increase in fatigue life at the same mean stress for the more work hardened 40% drawn rod at elevated stress levels. At lower stress levels the results overlap and show no significant difference in fatigue life. When adjusted for a percentile of yield stress percentile the 10% drawn rod outperforms the 40% drawn rod. It is theorized that this may be due to a increase in brittleness or the increased relative size of the notch on the 40% drawn rod.

-Is there any correlation between the fracture mode and fatigue life?

The fatigue initiation site revealed an influence on the fatigue life of the samples. With the same loads and samples initiation at the notch edge compared to the center led to a doubling of fatigue life for some test subsets. This is reasoned to be caused by the geometry of the notching tool and alignment issues during the notching process.

-Can trends in fatigue life be evaluated using a Junker's testing machine?

With the equipment available, the Junker's testing machine is only suitable for fatigue testing of fasteners. Furthermore, the limited testing performed on fasteners

can only provide information about the failure mode and location, and not the fatigue life.

Bibliography

[1] *Mechanical properties of fasteners made of carbon steel and alloy steel - Part 1: Bolts, screws and studs with specified property classes - Coarse thread and fine pitch thread*. Standard. Geneva, CH: International Organization for Standardization, Jan. 2013.

[2] G.E. Totten, K. Funatani, and L. Xie. *Handbook of Metallurgical Process Design*. Marcel Dekker inc, 2004. ISBN: 0-8247-4106-4.

[3] Bruce Boardman. *Fatigue Resistance of Steels*. ASM International, Jan. 1990. ISBN: 978-1-62708-161-0. DOI: 10.31399/asm.hb.v01.a0001038. eprint: https://dl.asminternational.org/book/chapter-pdf/445906/a0001038.pdf. URL: https://doi.org/10.31399/asm.hb.v01.a0001038.

[4] M.A. Meyers and K.K. Chawla. *Mechanical Behavior of Materials*. Cambridge University Press. ISBN: 9781107394186.

[5] ASM Handbook Committee. *Fatigue and Fracture*. ASM International, Jan. 1996. ISBN: 978-1-62708-193-1. DOI: 10.31399/asm.hb.v19.9781627081931. URL: https://doi.org/10.31399/asm.hb.v19.9781627081931.

[6] S. Lampman. "Intergranular Fracture". In: *Failure Analysis and Prevention*. ASM International, Jan. 2002. ISBN: 978-1-62708-180-1. DOI: 10.31399/asm.hb.v11.a0003540. eprint: https://dl.asminternational.org/book/chapter-pdf/435147/a0003540.pdf. URL: https://doi.org/10.31399/asm.hb.v11.a0003540.

[7] J. C. Pang et al. "Relations between fatigue strength and other mechanical properties of metallic materials". In: *Fatigue & Fracture of Engineering Materials & Structures* 37.9 (2014), pp. 958–976. DOI: https://doi.org/10.1111/ffe.12158. URL: https://onlinelibrary.wiley.com/doi/abs/10.1111/ffe.12158.

[8] Mohamed Sadek et al. "20 kHz 3-point bending fatigue of automotive steels". In: *MATEC Web of Conferences* 165 (Jan. 2018), p. 22020. DOI: 10.1051/matecconf/201816522020.

[9] *Standard Practice for Statistical Analysis of Linear or Linearized Stress-Life (S-N) and Strain-Life (ϵ-N) Fatigue Data*. Standard. Pennsylvania, USA: American Society for Testing and Materials, 2015.

[10] W.D. Pilkey and R.E. Peterson. *Peterson's Stress Concentration Factors*. A Wiley-Interscience publication. Wiley, 1997. ISBN: 9780471538493. URL: https://books.google.se/books?id=Nr1RAAAAMAAJ.

[11] Ruitao Qu, Peng Zhang, and Zhefeng Zhang. "Notch Effect of Materials: Strengthening or Weakening?" In: *Journal of Materials Science & Technology* 30.6 (2014), pp. 599–608. ISSN: 1005-0302. DOI: https://doi.org/10.1016/j.jmst.2014.04.014. URL: https://www.sciencedirect.com/science/article/pii/S1005030214000723.

[12] Joachim Rösler, Harald Harders, and Martin Bäker. *Mechanical behaviour of engineering materials: metals, ceramics, polymers, and composites*. Springer Science & Business Media, 2007.

[13] George F. Vander Voort. *Visual Examination and Light Microscopy*. ASM International, Jan. 1987. ISBN: 978-1-62708-181-8. DOI: 10.31399/asm.hb.v12.a0001834. eprint: https://dl.asminternational.org/book/chapter-pdf/490923/a0001834.pdf. URL: https://doi.org/10.31399/asm.hb.v12.a0001834.

[14] Nord-Lock Group. *Introducing the Junker test*. URL: https://www.nord-lock.com/insights/knowledge/2010/introducing-the-junker-test/ (visited on 01/31/2023).

[15] *Aerospace series — Dynamic testing of the locking behaviour of bolted connections under transverse loading conditions (vibration test)*. Standard. Geneva, CH: International Organization for Standardization, Aug. 2015.

A
Appendix

In this chapter images and tables of some interest that are not directly necessary to grasp the work performed in the report is included for interested readers.

Table A.1: Chemical composition of the material 22MnB5Ti.

C	Si	Mn	P	S	Cr	Ni	Mo	Cu	Al	Ti	V
0,233	0,477	1,249	0.013	0.005	0.284	0.019	0.002	0.023	0.034	0.026	0.002

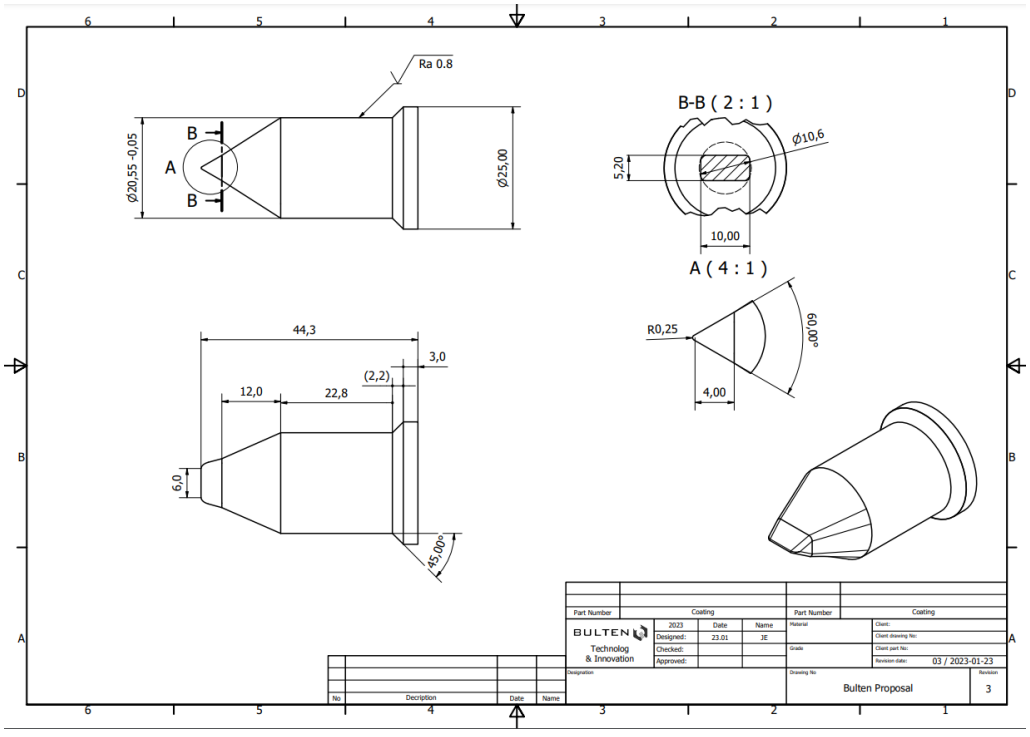

Figure A.1: Close up of inclusion, with a scale bar of 0.01mm.

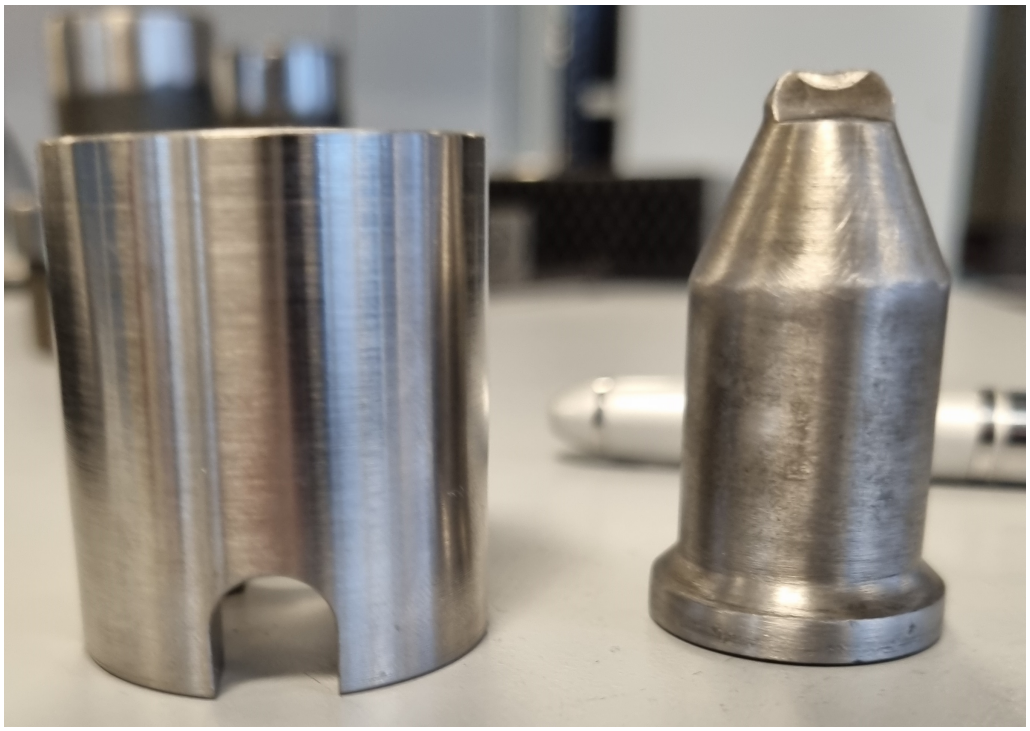

Figure A.2: Notching tool, holder on the left with indent tool on the right.

Table A.2: Fatigue fracture initiation point,
LEGEND
A= Initiation site in central part of notch.
B = Initiation site in between edge and center.
C = Initiation site at edge.
D = Unique form, initiation at both edges.

10% drawn rods		40% drawn rods	
YS & Cycle number	Fracture type	YS & Cycle number	Fracture type
50YS_1527k	C	50YS_209.6k	D
50YS_362.5k	C	50YS_311.3k	B
50YS_257.5k	C	50YS_206.7k	B
50YS_261k	C	50YS_214.8k	B
50YS_659.4k	D	50YS_202.8k	B
50YS_401.8k	D	50YS_444k	C
		50YS_332.7k	C
60YS_167.1k	A	50YS_588.8k	C
60YS_222.2k	C		
60YS_177.5k	B	60YS_88.4k	B
60YS_193.8k	B	60YS_126.8k	D
		60YS_93.3k	B
70YS_54.2k	B		
70YS_74.6K	A	70YS_32.3k	A
70YS_72.8k	A	70YS_43.1k	A
70YS_63.2k	B	70YS_34.7k	A
		70YS_31k	A
80YS_41.3k	A	80YS_20.6k	A
80YS_25.7k	A		
		Extra_49.3k	C
Extra_9.39k	A	Extra_33.1k	B
Extra_8.76k	A	Extra_30.7k	C
Extra_9.1k	A	Extra_39.4k	D
Extra_9.34k	A		

Table A.3: Measured notch data, including samples pre-measured and those only measured after fracture. Showing some variation in notch depth.

Pre-measured			Notch depth		Notch depth	
Sample	Before	After	Before	After	Before	After
#2_40_202.8k	6.05	6.050	0.95	0.950	0.95	0.95
Weak_notch_10_33k	7.83	7.798	0.67	0.703	0.67	0.7025
Weak_notch_40_58.08k	6.22	6.175	0.78	0.825	0.78	0.825
#9_10_322.7k	7.66	7.690	0.84	0.810	0.84	0.81
#3_10_588.8k	7.67	7.635	0.83	0.865	0.83	0.865
#5_10_444k	7.64	7.645	0.86	0.855	0.86	0.855

Not-pre-measured						
			Notch depth		Notch depth	
Sample	Before	After	Before	After	Before	
10_25.7k	N/A	7.672	0.828		0.828	
10_193.8k	N/A	7.676	0.824		0.824	
10_257.5k	N/A	7.6415	0.8585		0.8585	
10_261k	N/A	7.7475	0.7525		0.7525	
10_1527k	MISALIGNED	N/A	N/A		N/A	
10_74.6k	N/A	7.685	0.815		0.815	
10_362.5k	N/A	7.7025	0.7975		0.7975	
10_222.2k	N/A	7.693	0.807		0.807	
10_177.5k	N/A	7.715	0.785		0.785	
10_659.4k	N/A	7.7325	0.7675		0.7675	
10_72.7k	N/A	7.8085	0.6915		0.6915	
10_63.2k	N/A	7.7905	0.7095		0.7095	
10_16.7k	N/A	7.7785	0.7215		0.7215	
10_41.3k	MISALIGNED	N/A	N/A		N/A	
10_54.2k	N/A	7.7565	0.7435		0.7435	
10_401.8k	N/A	7.707	0.793		0.793	

Figure A.3: Close up of inclusion, with a scale bar of 0.01mm.

B

Investigating the use of a Junkers machine to evaluate fatigue life

This appendix is dedicated to the investigation carried out regarding the potential to use the Junkers machine to perform expedient fatigue life testing. It encapsulates everything from the machine and its function to the results gathered during the project.

B.1 Junker's machine

The Junker vibration test is a experiment designed in the 1960s to measure the self-loosening behaviour of bolts when exposed to vibrations. The test uses transverse loading at a right angle to the fastened bolt which induces vibrations causing loosening [14]. This test is standardized as DIN 65151 (ISO 16130). [15]

A Junker's test machine is a test rig designed for this purpose. The rig allows mounting of bolts and having a means of applying transverse loading and measuring clamping force. By mounting a thin rod centered around the transverse load it is theorized that a fatigue failure can be induced in the material.

B.2 Testing method

To mount the drawn rods in the Junkers testing machine, specialized grips had been designed by Bulten before the start of the project. These grips allowed fixation of the free end of the test piece, the grips, and the test piece itself can be seen in Fig. B.1 marked as #5, #6 and #8. The bisected cylinder grip is fastened inside the mounting sleeve (#7) by several set screws. A schematic illustration of the assembled parts can be seen in Fig. B.2

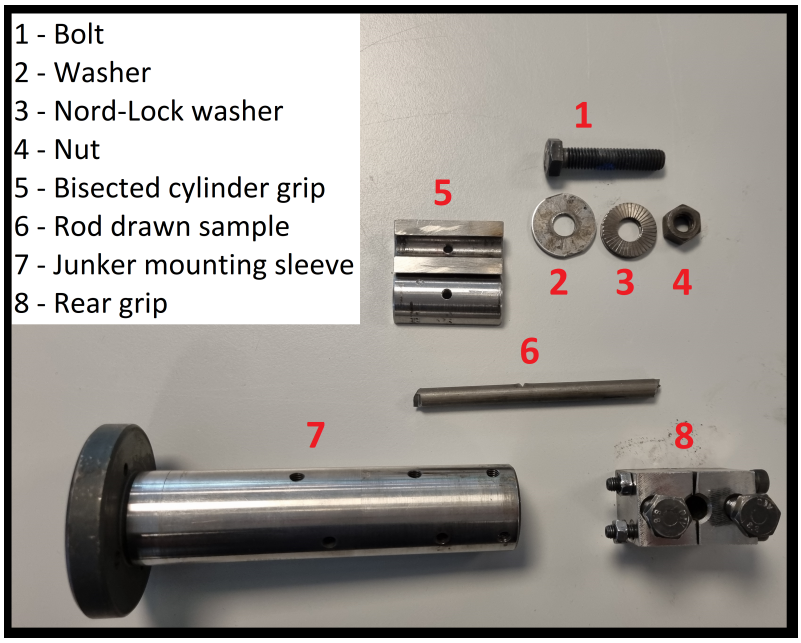

Figure B.1: Junker material and test equipment.

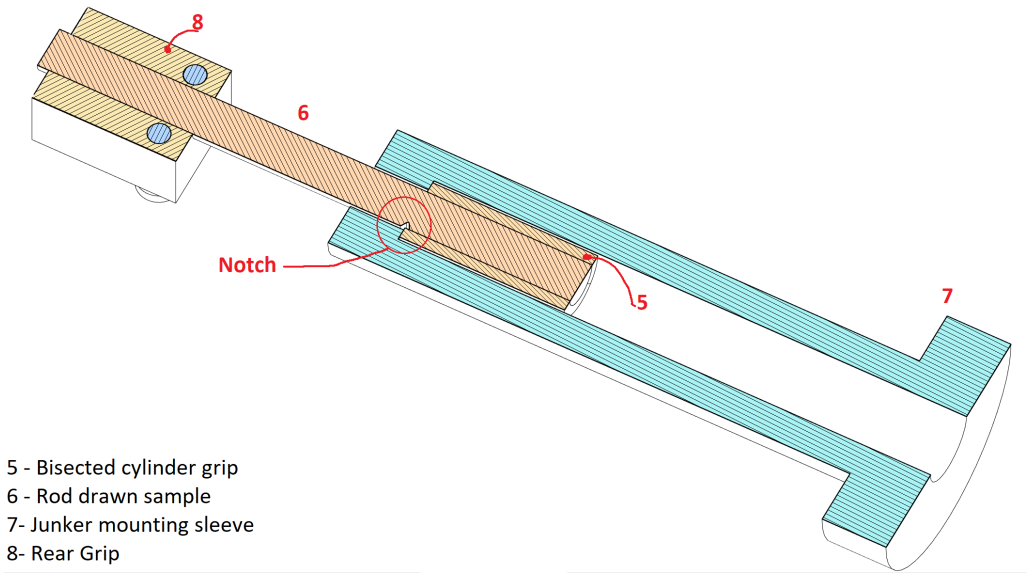

Figure B.2: Section view of assembled junker testing equipment.

After a initial test series it became apparent that the bisected cylinder grip did not allow for sufficient gripping force on the smaller diameter samples. As a result these samples would often shake loose before testing could be concluded. To remedy this, additional grips were manufactured for each diameter, with the addition of set

screws in the grips to achieve better gripping strength.

With the new grips further testing could be performed, in order to determine the site of fracture. Initially the notch was placed centrally on the test piece, however fracture would occur at either grip instead of the notch, as seen in Fig. B.3. Thereafter the notch was placed at either grip, and it was determined that the site with the highest stress was at the end of the bisected cylinder grips, as such notches were placed there in future testing.

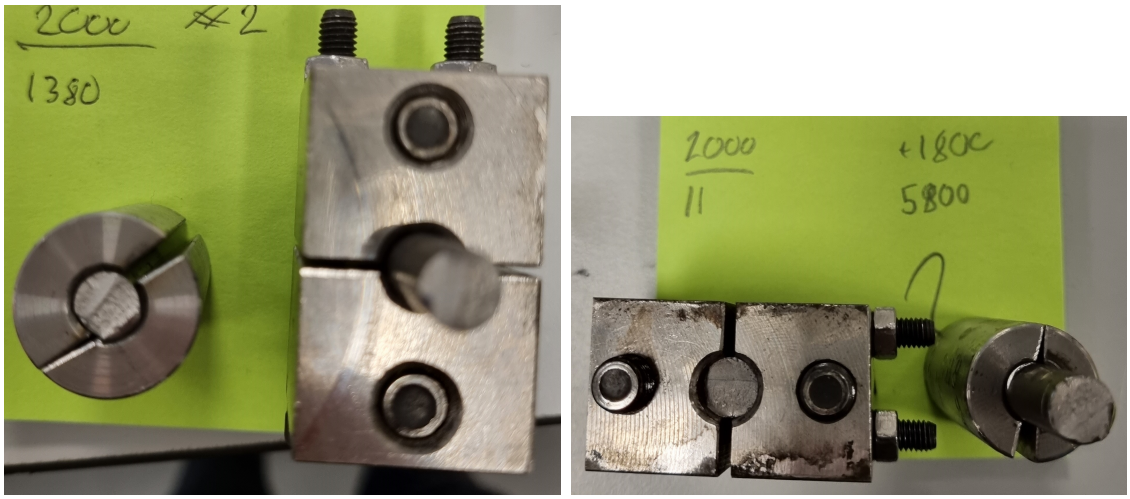

(a) Fracture at bisected cylinder grip. **(b)** Fracture at rear grip.

Figure B.3: Comparison of different fracture sites in Junker tests.

While the new grips allowed some testing of the drawn rods to be performed, many issues still remained. Loosening of the samples still occurred, leading to repeated canceled tests. Additionally, the setup did not allow for measurement of the clamping force, as such the determining the moment of fracture required constant monitoring of the machine and manual termination of testing. Furthermore software instability at high cycle numbers resulted in repeated failed tests, requiring additional manual intervention.

Due to these factors the testing approach had to be reexamined. The Junker machine is designed for the testing of fasteners, and as the testing of fasteners would be more applicable for Bulten, attempts to compare the rod drawn samples using the Junkers machine was abandoned in favor of testing finished fasteners.

Finished fasteners were mounted in the Junkers machine as a bolted joint with a fresh Nord-Lock washer for each test to prevent self-loosening of the fastener. Reference 10.9 bolts were tested against varying prototype versions of BUFOe fasteners available.

The fasteners were mounted in the Junkers machine as a bolted joint, consisting of a fastener, washer, Nord-Lock washer and a nut placed in the rear sleeve. This was

then torqued to a specified clamping force. Initial testing showed a strong connection between clamping force and cycles to failure. A torqued clamping force of 8kN was chosen as a target value, being easier to consistently torque while preventing self-loosening in combination with the Nord-Lock washer. The test itself was ran at a set amplitude of 0.7mm at 12.5 Hz.

B.3 Results & Discussion

The data gathered for the tested fasteners in the Junkers machine can be seen in Table. B.1. Showing number of cycles, torque, clamp force loaded to and the final fracture location. Three types of fasteners were tested; (1) reference standard 10.9 fasteners, (2) BUFOe 1000 standard and (3) bake hardened versions of BUFOe 1000. No difference in average cycles to failure could be established between the three types of fasteners, additionally a large spread was observed.

Table B.1: Fatigue data gathered from Junker fatigue testing.

Reference 10.9				
#	Cycles	Torque [Nm]	Initial clamp force [kN]	Fracture location
1	2594	45.5	8.1	Thread
2	2961	40.8	8.6	Thread
3	2092	41.4	8.5	Thread
4	3685	28.5	8.7	Thread
5	1723	29.7	8.1	Thread
BUFOe1000				
1	2914	28.3	8.2	Thread
2	2560	32.4	8.9	Under head
3	2097	30.7	8.1	Under head
4	4077	30.2	8.9	Thread
5	1361	34.3	8.7	Under head
BUFOe1000 bake hardened				
1	1964	45.1	8.1	Under head
2	2065	40.2	8.2	Under head
3	3272	38.7	8.2	Under head
4	3514	42.7	8.1	Thread
5	2773	41	8	Under head

The number of cycles to failure shown in the data places the testing in the low cycle fatigue region. Fig B.5 shows a preliminary test performed at higher amplitude and clamping force. In Fig B.5 a decrease in clamping force during the test can be seen, this is likely due to plastic deformation of the sample. Furthermore, the shape of the curve just before failure is indicative of the failure mode. The sharp drop shown

for the BUFOe 1000 samples corresponds to brittle failure directly under the head. The reference 10.9 bolts show a more gradual decline, the fracture sites for these are shown in Fig. B.4.

(a) Reference bolt fractures.

(b) BUFOe 1000 fractures.

(c) Bake hardened BUFOe 1000 fractures.

Figure B.4: Comparison of different bolt failure sites from Junker testing.

The trend of the BUFOe bolts to fracture under the head as compared to the threads is undesirable as brittle fracture is more likely to result in catastrophic failure. The probable explanation of this failure mode is the combination of residual tensile stresses and locally elevated hardness, both resulting from the forging operation. These local defects are not present in the reference bolts as they are heat treated.

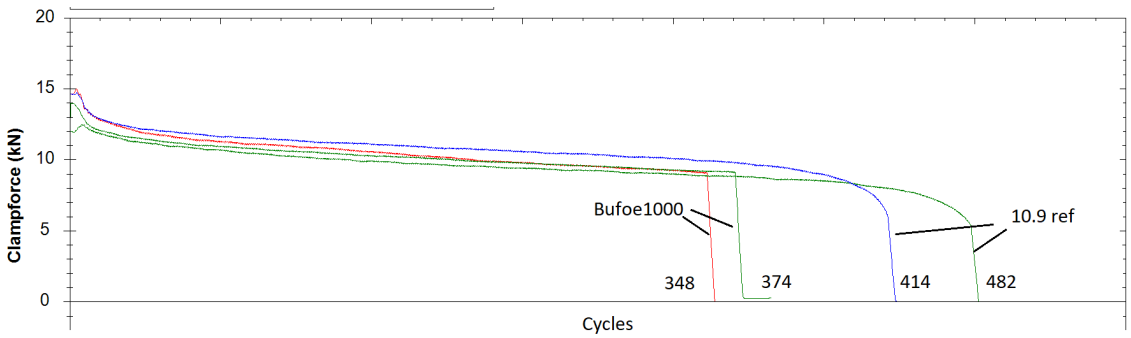

Figure B.5: Example of resulting data from fastener testing in Junkers machine.

B.4 Conclusion

Testing using rods proved inconclusive due to the numerous challenges outlined in the previous section. Given the constraints associated with testing rods it can be concluded that this type of testing is not feasible given the available equipment for mounting and and software to control the tests.

The use of fasteners when testing fatigue proved more fruitful with the Junkers machine, as compared to the drawn rods. However determining differences in fatigue life with the coarse load of the Junker machine is difficult. A difference in the failure site can be seen from the limited testing performed in this chapter, yet no conclusion of fatigue life can be drawn.

Further testing at lower amplitudes and with larger sample sizes may result in a clearer difference in fatigue life, however given the aforementioned software instabilities longer tests are challenging.

DEPARTMENT OF INDUSTRIAL AND MATERIALS SCIENCE
CHALMERS UNIVERSITY OF TECHNOLOGY
Gothenburg, Sweden
www.chalmers.se

CHALMERS
UNIVERSITY OF TECHNOLOGY